Open Access

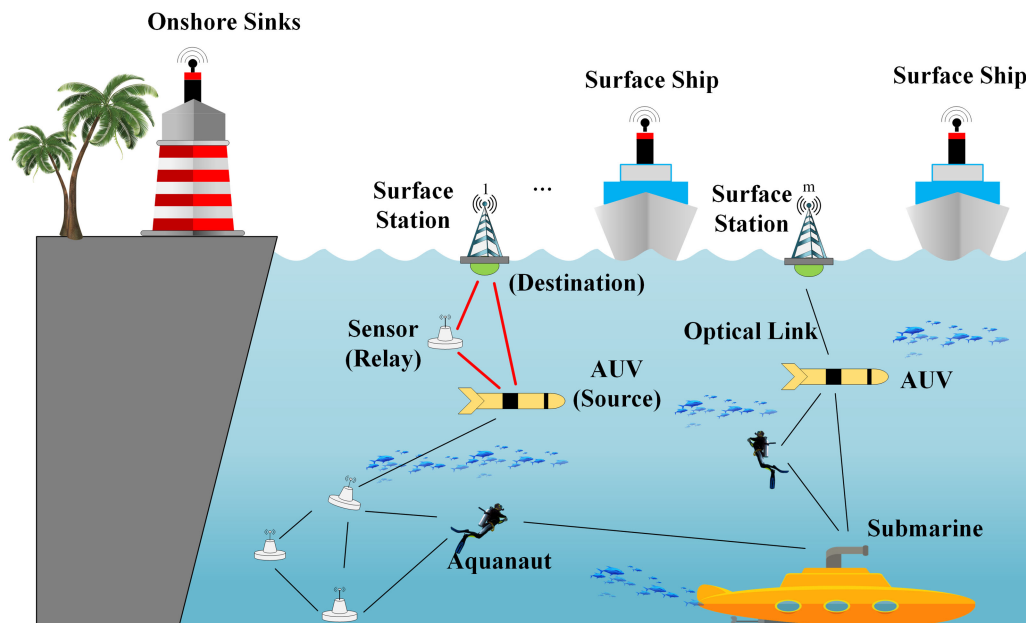# Performance Analysis for Cooperative Communication System in Optical IoUT Network With HDAF Strategy

Shuang Li
Ping Wang
Weina Pang
Wei Wang
Lixin Guo, *Member, IEEE*

Performance Analysis for Cooperative Communication System in Optical IoUT Network With HDAF Strategy

Shuang Li,[1] **Ping Wang** ⓘ**,**[1] **Weina Pang,**[1] **Wei Wang,**[1]
and Lixin Guo ⓘ**,**[1,2] *Member, IEEE*

[1]State Key Laboratory of Integrated Service Networks, School of Telecommunications
Engineering, Xidian University, Xi'an 710071, China
[2]School of Physics and Optoelectronic Engineering, Xidian University, Xi'an 710071, China

Abstract: In this work, a cooperative optical Internet of Underwater Things (IoUT) system with hybrid decode-amplify-forward (HDAF) strategy is first proposed and investigated over the aggregated underwater wireless optical communication (UWOC) channel. The impacts of absorption, scattering and the misalignment caused by spatial spreading in the sea, which are modeled by the beam spread function (BSF), as well as the oceanic turbulence on the underwater optical links are all included to describe the practical channel characteristics. With the help of Gauss-Hermite and Gauss-Legendre quadrature numerical methods, the closed-form expressions of the average bit error ratio (ABER) and outage probability for this cooperative optical HDAF-IoUT system are derived and verified by the Monte Carlo (MC) simulations. Furthermore, numerical analyses are offered to explore the effects of water type, turbulence strength, relay location and power allocation scheme on this HDAF-IoUT system. The performance of this optical system over the mixture Exponential Generalized Gamma (EGG) channel is also given for comparison. The obtained results indicate that the optical HDAF-IoUT system is superior to the IoUT system with fixed amplify-and-forward (FAF) strategy, and has a better performance when the relay is close to the middle position for a fixed power allocation scheme. This work is beneficial for the cooperative system design in IoUT network.

Index Terms: Internet of Underwater Things, hybrid decode-amplify-forward, underwater wireless optical communication, beam spread function.

1. Introduction

As is known, more than 70% of the earth's surface is covered by water which nurtures life on the earth and regulates its climate [1], [2]. With the development of science and technology and resource depletion on the land, the exploitation and utilization of the ocean is extremely urgent. However, the complexity of underwater environment has brought great difficulties for people to explore marine resources [3]. The Internet of Underwater Things (IoUT) could provide a possible means to address these questions [4]. IoUT is a novel class of Internet of Things, which is defined as the network of smart interconnected underwater objects. It is expected to enable various practical applications, such as environmental monitoring, coastal surveillance, navigation,

and underwater exploration [5]. Obviously, the efficient communication between different entities of IoUT networks is a fundamental and critical issue. Existing IoUT networks generally use the underwater wireless communication (UWC) technology based on radio frequency (RF), acoustic and optical waves *et al.* wireless carriers to transmit information [1], [6]. In fact, since RF wave would be severely attenuated in the sea water, it is seldom adopted in UWC system. Underwater wireless acoustic communication (UWAC) technique has become a welcoming solution for long-distance transmission in IoUT network [7]. However, long propagation delay, high signal attenuation, and low transmitting rate etc. limitations would lead to tremendous challenges in UWAC network design [8]. Comparing with RF communication and UWAC techniques, underwater wireless optical communication (UWOC) technique can not only achieve Gbps data rate within few hundreds of meters but also have better security and more flexible deployment. Those advantages make it become one of the potential alternatives to achieve data transmission in the IoUT network [9]. Nevertheless, the current development of UWOC technology would be restricted by the absorption, scattering, link misalignment and oceanic turbulence.

Absorption and scattering are two different effects of the same phenomenon, i.e., interaction of light photons with particulate matter and water molecules would lead to path loss, deviation of photons, and degradation in received power [10]. These two factors are generally described by the well-known Beer-Lambert's law [11]. However, this method is imprecise because only the ballistic photons are considered, which will severely underestimate the received power especially in the scattering water column [12]. Actually, a well-collimated laser beam may be largely diffused in space when it reaches the receiver due to the particulate scattering in natural waters. Hence, it is quite essential to investigate the misalignment of UWOC link caused by spatial spreading of optical beams. In the present works, ray tracing simulation is a quite popular method to characterize the UWOC channel, which simulates the trajectories of numerous photons under the consideration of water types, link distances and transceivers parameters [12]–[14]. The ray tracing method provides a more realistic underwater channel model than the Beer-Lambert's law, but its computational complexity is very large [14]. Recently, beam spread function (BSF) model has been proposed to characterize the misaligned UWOC link which includes a combined effect of two independent phenomena, absorption, scattering and the misalignment caused by spatial spreading in a single equation [15], [16]. In [15], B. M. Cochenour *et al.* introduced the theory used to solve radiative transport equation (RTE) and derived the analytical expression of BSF model, which has been validated via laboratory experiments. In [16], S. Tang *et al.* investigated the performance of the misaligned UWOC systems considering the BSF model. Numerical results indicated that under given transmitting power and link range, an appropriate offset distance between transmitter and receiver would not seriously reduce the performance of UWOC systems. Furthermore, the BSF model gives a relatively accurate analytical solution, which could be computed very quickly with greater flexibility. Thus this model is adopted to characterize the impact of absorption, scattering and the misalignment caused by spatial spreading on the UWOC link in this work. Aside from absorption, scattering and link misalignment, oceanic turbulence in the UWOC channels is also an extremely important factor [17]–[20]. So far, various statistical distributions for the turbulence-induced fading have been presented to describe the intensity fluctuations of optical beams in the presence of temperature, salinity, and air bubbles [21], such as lognormal (LN) distribution, Gamma Gamma (GG) distribution, and the mixture EGG distribution, etc. These statistical distributions have been verified through experiments in the water tank [21]–[23]. Among them, LN distribution is the most mature model and has been widely employed to characterize the turbulence-induced fading in UWOC channels under weak turbulence [18], [19].

In order to remove these impediments and extend the viable communication range of UWOC system, the averaging-aperture, spatial diversity, channel coding and relay-assisted etc. techniques have been proposed in [18]–[20], [22]–[25]. Motivated by the fact that there are numerous underwater objects interconnected with each other in optical IoUT network, the relay-assisted cooperative communication technique is a promising way to improve UWOC system performance. Cooperative transmission, which adopts spare transceivers of other nodes in the network to assist data transmission, has the abilities to extend the communication range and provides spatial diversity gain [26].

In cooperative communication scheme, amplify and forward (AF) and decode and forward (DF) are two most common protocols, which have been extensively used in wireless optical communication systems [27]. Concretely, AF protocol refers that relay terminals simply amplify the received signals without performing any sort of signal regeneration. A disadvantage of AF protocol is the noise amplification, which is incurred by the relay's action. Meanwhile, one notable advantage is able to operate at all times, including when the source-relay channel experiences outage [28]. The performance of the cooperative systems employing AF relaying scheme has been studied over the Rayleigh fading channels [29], [30]. In addition, the authors also analyzed the effects of co-channel interference and the optimal power scheme on the performance of cooperative diversity networks with AF strategy [31], [32]. For DF protocol, the relay fully decodes and re-decodes the received signals in turn and then transmits a new message to the destination. Severe performance degradation would be caused if the relay wrongly decodes the signals. However, when the instantaneous source-relay channel is suitable for a clean data extraction, DF protocol would perform better since it regenerates and passes on a clean set of signals. In [33] and [34], the error performance and outage performance of a single-relay cooperative system were comprehensively investigated for DF relaying over the Nakagami-m fading channels. Furthermore, DF protocol could be classified as fixed DF (FDF) protocol and adaptive DF (ADF) protocol, which is also known as selective DF protocol. In FDF strategy, the relay just decodes, re-decodes the received signals and then forwards new messages. In [35], focusing on the worst scenarios, it was found that the performances of FDF and AF strategy are not much different, and they are pretty bad for both cases. Comparing with FDF strategy, the selective DF strategy would decide whether it is necessary to forward the received signals by evaluating the quality of the received signals with a predefined metric such as a certain SNR threshold. The performance of the selective DF protocol is investigated in [36] and the author proposed an SNR optimal threshold to minimize the average bit error rate (ABER). In [37], the impact of the relay placement on the diversity order in adaptive selective DF cooperative strategies is investigated in the context of free-space optical (FSO) communication over atmospheric turbulence channels with pointing errors when line of sight is available. In [38], the performance of a selective DF relaying based multiple-input multiple-output (MIMO) space-time block coded (STBC) cooperative communication system with single and multiple relays is considered. Then, a hybrid decode-amplify-forward (HDAF) protocol is proposed, which combines both ADF and AF protocols to further improve the system performance [39], [40]. It was found that HDAF outperforms ADF and AF strategies HDAF in terms of symbol error performance, and the performance gain depends on the relay's location. In [41], H. Xiao *et al.* provided error performance analysis and minimum power allocation for multi-source multi-destination cooperative vehicular networks using the HDAF cooperative relaying protocol. In [42], H. Khanna *et al.* presented the performance of a dual-hop mixed RF-FSO system employing HDAF strategy. Results indicated that HDAF relaying in a mixed RF-FSO system could obviate the need for a direct LOS link between the source and the destination ends. In [43], the outage performance of mobile-to-mobile (M2M) cooperative networks employing HDAF relaying scheme was investigated over N-Nakagami fading channels. Results revealed that the fading coefficient, number of cascaded components, relative geometric gain, and power-allocation are important parameters that would influence the outage probability. In [44], S. Abdelhamid *et al.* investigated non-orthogonal multiple access (NOMA) for a cooperative wireless relaying system over Rayleigh fading channels, which reveals that the location of the relay is the key parameter to achieve the best performance. However, to the best of our knowledge, there are no reports that address cooperative relaying strategy for IoUT networks over the underwater wireless optical channels up to now. Since the channel model of UWOC system is distinctive, the existing achievements obtained in RF wireless communication system and FSO communication system could not be applicable for UWOC systems directly. The absorption, scattering, oceanic turbulence, and link misalignment between the transceivers of seawater would deteriorate the system performance, which should be comprehensively considered in UWOC channels. Therefore, this work intends to conduct a comprehensive investigation on the ABER and outage performances analysis of the cooperative optical IoUT system over UWOC channels.
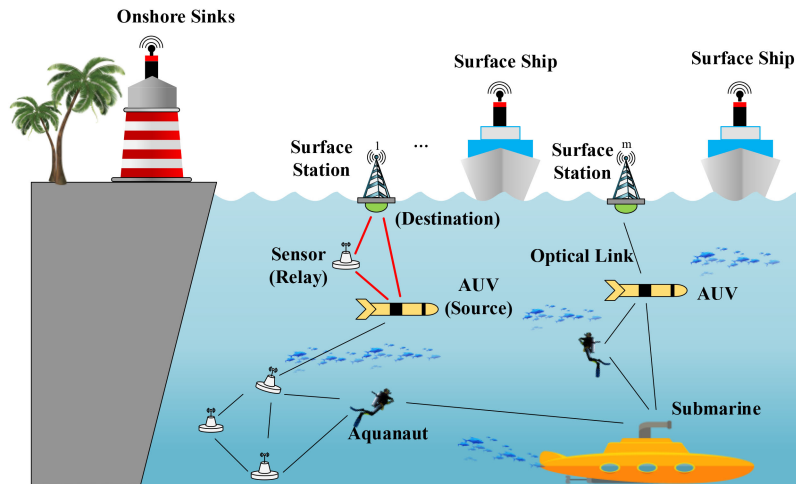
Fig. 1. Architecture of the cooperative optical IoUT network.

In this paper, a cooperative optical IoUT system employing hybrid decode-amplify-forward transmission scheme is presented and investigated over the aggregated UWOC channel for the first time. The impacts of absorption, scattering and the misalignment caused by spatial spreading in the sea, which are modeled by BSF, as well as the oceanic turbulence on the underwater optical links are all included to describe the practical channel characteristics. The closed-form expressions of the ABER and outage probability for the HDAF-IoUT system are derived. The insights into the effects of power allocation schemes and relay locations on the error and outage performance of the optical IoUT system are also provided. Moreover, the performance of the cooperative optical HDAF-IoUT system over the aggregated EGG channel is given for comparison. The remainder of the paper is organized as follows: Section 2 depicts the cooperative optical HDAF-IoUT system model and the aggregated UWOC fading channel. In Section 3, metrics of system performance such as ABER and outage probability of the HDAF-IoUT system are presented. Subsequently, the analytical and MC simulation results are discussed in Section 4 and the paper is concluded in Section 5.

2. System and Channel Model

2.1 System Description

The architecture of the cooperative optical IoUT network with M surface stations and N static smart objects/nodes which can be underwater sensors using optical waves for communications is shown in Fig. 1. These smart objects interconnect with each other and they could be different types of underwater sensors, autonomous underwater vehicles (AUVs), submarines, ships, buoys, etc. In the process of information transmission, the sensory data from the IoUT devices is first forwarded to neighboring underwater nodes. And then these messages are sent to the water surface receiver in hop-by-hop and cooperative fashions via these moored smart objects [45].

In this work, we focus attention on a three-node half-duplex cooperative optical IoUT system with HDAF strategy, which consists of a source node (node S_i), a neighboring node (relay R_j) and a destination node (node D_k). Assumed that the channel state information could be available at the relay nodes and destination nodes by using the training sequence [46]. The HDAF strategy in the cooperative optical IoUT system mainly consists of two transmission phases. During the first phase, the source node transmits the message to R_j and D_k by using separate transmitter. The signals received at the relay and destination can be denoted as

$$y_{S_i R_j} = \sqrt{P_S}\eta h_{S_i R_j}x + n_{S_i R_j}, \tag{1}$$

$$y_{S_i D_k} = \sqrt{P_S}\eta h_{S_i D_k} x + n_{S_i D_k}, \tag{2}$$

where $h_{S_i R_j}$ and $h_{S_i D_k}$ are independent complex channel coefficients of $S_i - R_j$ and $S_i - D_k$ links, respectively. x is the transmitting signal from the source node S_i with unit average power P'. P_S is the transmitting power of the node S_i. $n_{S_i R_j}$ and $n_{S_i D_k}$ represent the additive white Gaussian noise (AWGN), which could be modeled by the signal-independent complex Gaussian random variables with zero mean and variance $\sigma^2 = N_0/2$, where N_0 is the single power spectrum density of the AWGN.

In the second phase, the relay R_j would carry out cooperative transmission and forward a new message to D_k. Before forwarding the message, R_j decides to adopt AF strategy or DF strategy based on the channel quality of $S_i - R_j$ link. If the instantaneous SNR of the $S_i - R_j$ link exceeds SNR_{sr}, which provides the minimum SNR for R_j to decode the received message from S_i successfully, R_j would decode the received message, recode and forward a new message. Otherwise, R_j will adopt the AF strategy. With DF strategy employed, at D_k, the signals from the relay can be expressed by

$$y_{R_j D_k}^{DF} = \sqrt{P_R}\eta h_{R_j D_k} \hat{x} + n_{R_j D_k} \tag{3}$$

where $h_{R_j D_k}$ is the complex channel fading coefficient of the $S_i - D_k$ link, $\hat{x}$ denotes the re-encode signals at R_j, and P_R is the transmitting power of the relay. $n_{R_j D_k}$ is the same as $n_{S_i R_j}$ and $n_{S_i D_k}$. When the AF strategy is employed, the received signals at the destination can be given as

$$y_{R_j D_k}^{AF} = G\sqrt{P_R}\eta h_{R_j D_k} y_{S_i R_j} + n_{R_j D_k} \tag{4}$$

where the amplification coefficient G is defined in [47]. And then, the destination D_k combines the data copies from the relay and the signals from source with the maximum-ratio-combining (MRC) technique and restores the original signal. Thus, the combining signal at the destination could be modeled by

$$y_{D_k} = \begin{cases} w_{R_j D_k} y_{R_j D_k}^{DF} + w_{S_i D_k} y_{S_i D_k}, & \text{with DF strategy} \\ w_{R_j D_k} y_{R_j D_k}^{AF} + w'_{S_i D_k} y_{S_i D_k}, & \text{with AF strategy} \end{cases} \tag{5}$$

where $w_{S_i D_k}$, $w'_{S_i D_k}$ and $w_{R_j D_k}$ are weighting coefficients. The end-to-end equivalent SNRs of the optical IoUT system under DF and AF strategies can be, respectively, given as

$$\mu_{DF} = \min\left\{\mu_{S_i R_j}, \mu_{R_j D_k} + \mu_{S_i D_k}\right\} \tag{6}$$

$$\mu_{AF} = \mu_{S_i D_k} + \frac{\mu_{S_i R_j}\mu_{R_j D_k}}{\mu_{S_i R_j} + \mu_{R_j D_k} + 1} \tag{7}$$

where $\mu_{S_i R_j}$, $\mu_{R_j D_k}$, and $\mu_{S_i D_k}$ are the instantaneous SNRs of the $S_i - R_j$, $R_j - D_k$ and $S_i - D_k$ links, respectively. Furthermore, when the cooperative optical HDAF-IoUT system operates under the intensity modulation/direct detection (IM/DD), the end-to-end instantaneous SNRs of the $S_i - R_j$, $S_i - D_k$ and $R_j - D_k$ links can be written as $\mu_{S_i R_j} = P_S\eta^2|h_{S_i R_j}|^2/N_0/2 = \bar{\mu}_{S_i R_j}|h_{S_i R_j}|^2$, $\mu_{S_i D_k} = P_S\eta^2|h_{S_i D_k}|^2/(N_0/2) = \bar{\mu}_{S_i D_k}|h_{S_i D_k}|^2$ and $\mu_{R_j D_k} = P_R\eta^2|h_{R_j D_k}|^2/N_0/2 = \bar{\mu}_{R_j D_k}|h_{R_j D_k}|^2$, respectively. $\bar{\mu}_{S_i R_j} = \bar{\mu}_{S_i D_k} = P_S\eta^2/N_0/2$ and $\bar{\mu}_{R_j D_k} = P_R\eta^2/N_0/2$ are the corresponding average electrical SNRs.

2.2 Channel Model

2.2.1 Absorption, Scattering and Misalignment: When the laser beam propagates through the UWOC channel, it suffers high attenuation and multiple scattering, which would limit the link range to hundred meters. Taking into account both attenuation and the impact of spatial spreading on the underwater optical links, the BSF model is employed to describe the UWOC link [16]. Under the assumption of the small angle approximation (SAA) and symmetric irradiance distribution, the irradiance distribution of the receiver plane perpendicular to the beam axis at $z = z_{rec}$ (Given that

TABLE 1
Typical Values of Absorption and Scattering Coefficients [12]

Water type	a (m^{-1})	b (m^{-1})	c (m^{-1})
Pure water	0.053	0.003	0.056
Clear water	0.114	0.037	0.151
Costal water	0.179	0.219	0.398

the transmitter is at the origin of the coordinates $z = 0$.) can be expressed as [15]

$$BSF(\delta, z_{rec}) = E_0(\delta, z_{rec}) \exp(-cz_{rec})$$

$$+ \frac{1}{2\pi} \int_0^\infty E_0(v, z_{rec}) \exp(-cz_{rec})$$

$$\times \left\{ \exp\left[\int_0^{z_{rec}} bp(v(z_{rec} - z))\,dz\right] - 1 \right\} J_0(vr)\,v\,dv \tag{8}$$

where $E_0(\delta, z_{rec})$ and $E_0(v, z_{rec})$ are the irradiance distributions of the laser source in spatial co-ordinate system (δ, z_{rec}) and spatial frequency domain (v, z_{rec}), respectively. c is the extinction coefficient, whose values can usually be expressed as the sum of absorption coefficient a and scattering coefficient b. Typical coefficient values of a, b and c are given in Table 1. δ is the distance of the receiver aperture center away from the beam axis on the receiver plane. When $\delta = 0$, the transmitter and receiver are perfectly aligned. The received optical power is normalized by the initial transmitting power. The attenuation of propagating signals induced by absorption, scattering and the misalignment for a point receiver can be expressed as

$$h^a = \overline{BSF}(\delta, z_{rec}) \tag{9}$$

2.2.2 Oceanic Turbulence and Statistical Models: Under the weak oceanic turbulence, the LN distribution model is often considered to characterize the turbulence-induced fading. The probability density function (PDF) is given in [21]–[22]

$$f(h^t) = \frac{1}{h^t\sqrt{2\pi\sigma_X^2}} \exp\left\{ -\frac{(\ln h^t - m_X)^2}{2\sigma_X^2} \right\} \tag{10}$$

where h^t represents the random attenuation caused by the oceanic turbulence, m_X and σ_X^2 are the log-amplitude mean and variance, respectively. To guarantee that fading neither amplifies nor attenuates the average power, the fading coefficients is normalized as $\mathbb{E}[h^t] = 1$ with $\mathbb{E}(\cdot)$ donating expectation, which implies that $m_X = -0.5\sigma_X^2$ [21]. For lognormal fading channel, the log-amplitude variance relates to the scintillation index as $\sigma_X^2 = \ln(1 + \sigma_I^2)$ [21]. With the help of Rytov theory, the scintillation index of the Gaussian beam on the receiver aperture D can be calculated by [19]

$$\sigma_I^2(D) = 8\pi^2 k^2 L \int_0^1 \int_0^\infty d\zeta \kappa d\kappa \, \Phi_n(\kappa) \times \exp\left\{ -\frac{L\kappa^2}{k(\Lambda_1 + \Omega_G)}\left[(1 - \bar{\Theta}_1\zeta)^2 + \Lambda_1\Omega_G\zeta^2\right] \right\}$$

$$\times \left\{ 1 - \cos\left[\frac{L\kappa^2}{k}\left(\frac{\Omega_G - \Lambda_1}{\Omega_G + \Lambda_1}\right)\zeta(1 - \bar{\Theta}_1\zeta)\right] \right\} \tag{11}$$

Here, $k = 2\pi/\lambda$ is the wave number at the wavelength λ, L is the propagation distance, ζ is the normalized path length. κ denotes the magnitude of the spatial frequency. $\Omega_G = 16L/kD^2$ is a nondimensional parameter characterizing the spot radius of the collecting lens, and $\Lambda_1 = \Lambda_0/(\Theta_0^2 + \Lambda_0^2)$, $\Theta_1 = \Theta_0/(\Theta_0^2 + \Lambda_0^2)$, $\bar{\Theta}_1 = 1 - \Theta_1$. $\Lambda_0 = L/(k\alpha_s^2)$ and $\Theta_0 = 1 - L/F_0$ are the normalized parameters of the Gaussian beam with $2\alpha_s^2 = W_0^2$, where W_0 is the beam spot radius and F_0 is the radius of curvature. It should be noted that the focal length is chosen as $F_0 \to \infty$ in this study, corresponding
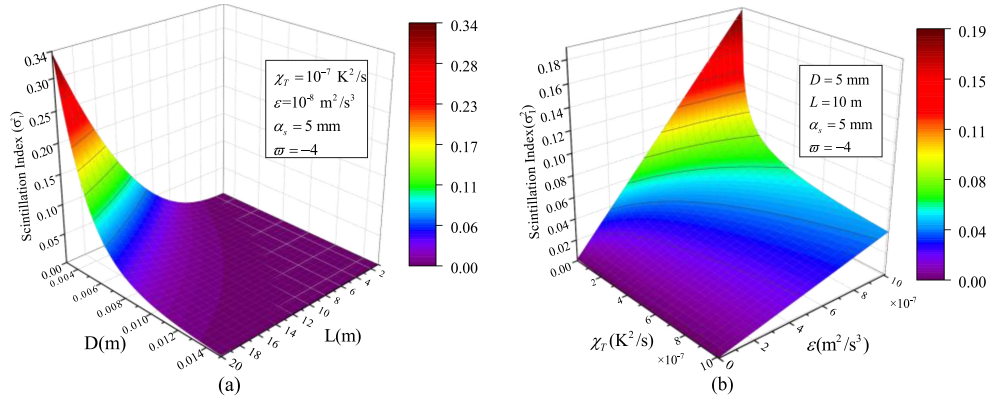
Fig. 2. Scintillation index versus (a) L and D, (b) χ_T and ε.

to the collimated optical Gaussian beam. $\Phi_n(\kappa)$ denotes the spatial power spectrum in locally homogeneous and isotropic oceanic turbulence at the stable stratification, which can be given by [18]

$$\Phi_n = (4\pi)^{-1} C_0 \alpha_0^2 \varepsilon^{-1/3} \kappa^{-11/3} \left[1 + C_1 (\kappa\eta)^{2/3}\right]$$

$$\times \frac{\chi_T}{\varpi^2} \left[\varpi^2 \exp(-A_T\delta) - 2\varpi \exp(-A_{TS}\delta) + \exp(-A_S\delta)\right] \quad (12)$$

where $A_T = C_0 C_1^{-2} D_T \upsilon^{-1}$, $A_{TS} = 0.5 C_0 C_1^{-2} (D_T + D_S) \upsilon^{-1}$, $A_S = C_0 C_1^{-2} D_S \upsilon^{-1}$, $\delta = 1.5 C_1^2 (\kappa\eta)^{4/3} + C_1^3 (\kappa\eta)^2$. $\alpha_0 = 2.56 \times 10^{-4} L/\text{deg}$ is a constant, $C_0 = 0.72$ is the Obukhov-Corrsin constant, and $C_1 \approx 2.35$ is the nondimensional constant determined by comparison with experiment data. The kinematic viscosity υ in water medium is much higher than the molecular thermal diffusivity D_T and the molecular salinity transport coefficient D_S. η is the Kolmogorov microscale. And ε is the rate of dissipation of turbulent kinetic energy per unit mass of fluid, which is in the range from $10^{-8} \text{m}^2/\text{s}^3$ to $10^{-2} \text{m}^2/\text{s}^3$. χ_T is the rate of dissipation of the mean squared temperature altering from $10^{-10} \text{K}^2/\text{s}$ to $10^{-2} \text{K}^2/\text{s}$. The quantity ϖ varies in the interval of $[-5, 0]$, defining the contributions of the temperature and salinity distributions to the distribution of the refraction index. Fig. 2 shows the variation of scintillation index with respect to system parameters. The 3D plot of scintillation index variation with L and D is illustrated in Fig. 2(a). The value of $\sigma_I^2(D)$ at $\chi_T = 10^{-7} \text{K}^2/\text{s}$, $\varpi = -4$, $\varepsilon = 10^{-8} \text{m}^2/\text{s}^3$, $\alpha_s = 5$ mm is 0.337. Fig. 2(b) represents the variation of scintillation index with χ_T and ε in the same way.

2.3 Statistics of Aggregated Channel

The probability distribution of the aggregated channel gain $h = h^a h^t$ can be expressed as

$$f(h) = \frac{1}{h\sqrt{2\pi\sigma_X^2}} \exp\left\{-\frac{\left[\ln h - \ln \overline{BSF}(\delta, z_{rec}) + 0.5\sigma_X^2\right]^2}{2\sigma_X^2}\right\} \quad (13)$$

The PDF of the instantaneous SNR when the cooperative optical IoUT system based on HDAF strategy operating under IM/DD can be given as

$$f(\mu) = \frac{1}{\mu\sqrt{2\pi\sigma_R^2}} \exp\left\{-\frac{\left[\ln \mu - \ln \bar{\mu} - 2\ln \overline{BSF}(\delta, z_{rec}) + \sigma_X^2\right]^2}{2\sigma_R^2}\right\} \quad (14)$$

where $\sigma_R^2 = 4\sigma_X^2$. Thus, the corresponding cumulative distribution function (CDF) can be achieved as

$$F_\mu(\mu) = \frac{1}{2} + \frac{1}{2} erf\left[\frac{\ln\mu - \ln\bar{\mu} - 2\ln\overline{BSF}(\delta, z_{rec}) + \sigma_X^2}{\sqrt{2\sigma_R^2}}\right] \tag{15}$$

3. Details Performance analysis of the Cooperative Optical HDAF-IoUT System

In this section, we aim to derive the closed-form expressions of the ABER and outage probability for the cooperative optical IoUT system on the basis of the HDAF strategy. The modulation schemes of the considering relay-assisted HDAF-IoUT system are binary phase shift keying (BPSK).

3.1 Average Bit Error Rate

According to the system model described in Section 2, in the cooperative transmission $S_i - R_j - D_k$ link, R_j forwards the data information to the destination D_k utilizing AF strategy, which only amplifies the received electric signals by a factor of G, when the instantaneous SNR of $S_i - R_j$ link is less than or equal to SNR_{sr}. Otherwise, R_j would employ the DF strategy, which decodes the received signals, re-encodes and forwards a new message to the destination D_k. Therefore, the ABER of the cooperative optical IoUT system over the UWOC channel in the case of HDAF scheme can be expressed as

$$P_{\mathsf{HDAF}}(e) = P\left(\mu_{S_i R_j} > SNR_{sr}\right) P_{DF}\left(e\middle|\mu_{S_i R_j} > SNR_{sr}\right)$$
$$+ P\left(\mu_{S_i R_j} \leq SNR_{sr}\right) P_{AF}\left(e\middle|\mu_{S_i R_j} \leq SNR_{sr}\right) \tag{16}$$

where $P_{DF}(e|\mu_{S_i R_j} > SNR_{sr})$ and $P_{AF}(e|\mu_{S_i R_j} \leq SNR_{sr})$ are the conditional error bit rate of the optical IoUT system when the relay adopts DF strategy and AF strategy, respectively. $P(\mu_{S_i R_j} > SNR_{sr})$ and $P(\mu_{S_i R_j} \leq SNR_{sr})$ are the probabilities of the relay node operating in DF mode and AF mode, respectively, which can be calculated as

$$P\left(\mu_{S_i R_j} > SNR_{sr}\right) = 1 - \frac{1}{2} erf\left[\frac{\ln(SNR_{sr}) - \ln\bar{\mu} - 2\ln\overline{BSF_{S_i R_j}}(\delta, z_{rec}) + \sigma_{S_i R_j}^2}{\sqrt{8\sigma_{S_i R_j}^2}}\right] \tag{17}$$

$$P\left(\mu_{S_i R_j} \leq SNR_{sr}\right) = \frac{1}{2} + \frac{1}{2} erf\left[\frac{\ln(SNR_{sr}) - \ln\bar{\mu} - 2\ln\overline{BSF_{S_i R_j}}(\delta, z_{rec}) + \sigma_{S_i R_j}^2}{\sqrt{8\sigma_{S_i R_j}^2}}\right] \tag{18}$$

The conditional ABER of the cooperative optical IoUT system in DF mode, $P_{DF}(e|\mu_{S_i R_j} > SNR_{sr})$, can be further expressed as

$$P_{ABER}^{DF}\left(e\middle|\mu_{S_i R_j} > SNR_{sr}\right) = P_{ABER}^{R}\left(e\middle|\mu_{S_i R_j} > SNR_{sr}\right) P_{ABER}^{prop}\left(e\middle|\mu_{S_i R_j} > SNR_{sr}\right)$$
$$+ \left[1 - P_{ABER}^{R}\left(e\middle|\mu_{S_i R_j} > SNR_{sr}\right)\right] P_{ABER}^{coop}\left(e\middle|\mu_{S_i R_j} > SNR_{sr}\right) \tag{19}$$

where $P_{ABER}^{R}(e|\mu_{S_i R_j} > SNR_{sr})$ is the detection error probability at the relay R_j, when the instantaneous SNR of the $S_i - R_j$ link is larger than SNR_{sr}. $P_{ABER}^{coop}(e|\mu_{S_i R_j} > SNR_{sr})$ is the conditional probability that an error occurs after the destination combines the signals from the source and the correctly detected signals from the relay, when $\mu_{S_i R_j} > SNR_{sr}$ holds on. And $P_{ABER}^{prop}(e|\mu_{S_i R_j} > SNR_{sr})$ represents the conditional probability of the error propagation event that an error occurs after the destination combines the signals from the source and the incorrectly detected signals from R_j. With BPSK modulation, the conditional detection error probability over the composite lognormal fading

channel can be expressed as

$$P_{ABER}^{R}\left(e|\,\mu_{S_iR_j} > SNR_{sr}\right) = \int_0^\infty Q\left(\sqrt{2\mu}\right)f_{S_iR_j}\left(\mu|\,\mu_{S_iR_j} > SNR_{sr}\right)d\mu \tag{20}$$

where $Q(.)$ is defined as $Q(x) = \int_x^\infty 1/\sqrt{2\pi}\exp(-t^2/2)dt$. $f_{S_iR_j}(\mu|\mu_{S_iR_j} > SNR_{sr})$ can be expressed as

$$f_{S_iR_j}\left(\mu|\,\mu_{S_iR_j} > SNR_{sr}\right) = \frac{\partial}{\partial\mu}\left[\frac{P\left(SNR_{sr} < \mu_{S_iR_j} \leq \mu\right)}{P\left(\mu_{S_iR_j} > SNR_{sr}\right)}\right]$$

$$= \begin{cases} \dfrac{f_{S_iR_j}(\mu)}{P\left(\mu_{S_iR_j} > SNR_{sr}\right)}, & \mu > SNR_{sr} \\ 0, & \mu \leq SNR_{sr} \end{cases} \tag{21}$$

Substituting Eq. (21) into Eq. (20), the conditional detection error probability can be calculated as

$$P_{ABER}^{R}\left(e|\,\mu_{S_iR_j} > SNR_{sr}\right) = \int_{SNR_{sr}}^\infty Q\left(\sqrt{2\mu}\right)\frac{f_{S_iR_j}(\mu)}{P\left(\mu_{S_iR_j} > SNR_{sr}\right)}d\mu$$

$$= \frac{1}{P\left(\mu_{S_iR_j} > SNR_{sr}\right)}\int_0^\infty Q\left(\sqrt{2\mu}\right)f_{S_iR_j}(\mu)\,d\gamma - \int_0^{SNR_{sr}} Q\left(\sqrt{2\mu}\right)f_{S_iR_j}(\mu)\,d\mu$$

$$= \frac{1}{P\left(\mu_{S_iR_j} > SNR_{sr}\right)}\left[I_1' - I_2'\right] \tag{22}$$

where $I_1' = \int_0^\infty Q(\sqrt{2\mu})f_{S_iR_j}(\mu)d\mu$, $I_2' = \int_0^{SNR_{sr}} Q(\sqrt{2\mu})f_{S_iR_j}(\mu)d\mu$. Gauss-Hermite quadrature (GHQ) rule [48] can be used to solve I_1' effectively. By converting the above integral I_1' to the standard form, it can be solved as follows

$$I_1' = \int_{-\infty}^\infty \frac{1}{2\sqrt{\pi}}\exp\{-t^2\}\,erfc\left(\sqrt{\exp\left(\sqrt{8\sigma_{S_iR_j}^2}\,t + u_{S_iR_j}\right)}\right)dt$$

$$\approx \sum_{l_1=1}^{L_1} H_{l_1} \times \frac{1}{2\sqrt{\pi}}erfc\left(\sqrt{\exp\left(\sqrt{8\sigma_{S_iR_j}^2}\,a_{l_1} + u_{S_iR_j}\right)}\right) \tag{23}$$

where a_{l_1} is the l_1th root of the Gauss-Hermite polynomial, H_{l_1} is the corresponding weight, and $u_{S_iR_j} = \ln\bar{\mu}_{S_iR_j} + 2\ln\overline{BSF_{S_iR_j}}(\delta, z_{rec}) - \sigma_{S_iR_j}^2$. And then, with the help of Eq. (24), Gauss-Legendre quadrature rule, the integral I_2' can be efficiently and accurately approximated [49]. The closed-form expression of I_2' can be calculated as Eq. (27).

$$\int_{-1}^1 g(\omega)\,d\omega = \sum_{k=1}^n S_k g(\omega_k) \tag{24}$$

$$S_k = \frac{2\left(1 - x_k^2\right)}{(n+1)^2(P_{n+1}(x_k))^2} \tag{25}$$

$$P_n(x) = \frac{1}{2^n}\sum_{k=0}^{[n/2]}(-1)^k\frac{(2n-2k)!}{k!(n-k)!(n-2k)!}x^{(n-2k)} \tag{26}$$

In Eq. (24), ω_k is the l_1th root of Legendre quadrature ($P_n(x) = 0$), which is given in Eq. (26), and n is the number of points.

$$I_2' = \int_0^{SNR_{sr}} Q\left(\sqrt{2\mu}\right)f_{S_iR_j}(\mu)\,d\mu$$

$$\approx \frac{SNR_{sr}}{2} \sum_{k_1=1}^{n_1} S_{k_1} \cdot \frac{1}{2} erfc \left(\sqrt{\frac{SNR_{sr}}{2} \omega_{k_1} + \frac{SNR_{sr}}{2}} \right)$$

$$\times \frac{1}{\sqrt{8\pi\sigma_{S_iR_j}^2} \left(\frac{SNR_{sr}}{2}\omega_{k_1} + \frac{SNR_{sr}}{2} \right)} \exp \left\{ -\left[\ln \left(\frac{SNR_{sr}}{2}\omega_{k_1} + \frac{SNR_{sr}}{2} \right) - u_{S_iR_j} \right]^2 \bigg/ \left(8\sigma_{S_iR_j}^2 \right) \right\} \quad (27)$$

Even if the relays can decode the sources' messages correctly, an error may also occur at the destination after combining the signals from the source and relay with MRC technique. The received SNR at the destination in DF mode can be written as $\mu_{coop} = \mu_{R_jD_k} + \mu_{S_iD_k}$, and then the PDF of μ_{coop} is denoted as $f_{coop}(x)$. This conditional error probability in the cooperative case with BPSK modulation can be calculated as

$$P_{ABER}^{coop} \left(e | \mu_{S_iR_j} > SNR_{sr} \right) = \int_0^\infty Q\sqrt{2\mu} f_{coop} \left(\mu | \mu_{S_iR_j} > SNR_{sr} \right) d\mu \quad (28)$$

where

$$f_{coop} \left(x | \mu_{S_iR_j} > SNR_{sr} \right) = \frac{\partial}{\partial x} \left[P \left(\mu_{R_jD_k} + \mu_{S_iD_k} < x | \mu_{S_iR_j} > SNR_{sr} \right) \right]$$

$$= \frac{\partial}{\partial x} \left[\frac{P \left(\mu_{R_jD_k} + \mu_{S_iD_k} < x, \mu_{S_iR_j} > SNR_{sr} \right)}{P \left(\mu_{S_iR_j} > SNR_{sr} \right)} \right]$$

$$= \frac{\partial}{\partial x} \left[P \left(\mu_{R_jD_k} + \mu_{S_iD_k} < x \right) \right]$$

$$= f_{coop} (x) \quad (29)$$

Submitting Eq. (29) into Eq. (28), $P_{ABER}^{coop}(e|\mu_{S_iR_j} > SNR_{sr})$ could be calculated with another standard method [50, Eq. (5)].

$$P_{ABER}^{coop} \left(e | \mu_{S_iR_j} > SNR_{sr} \right) = \int_0^\infty Q\sqrt{2\mu} f_{coop} (\mu) d\mu$$

$$= \frac{1}{\pi} \int_0^{\pi/2} M_\mu \left(-1/\sin^2\theta \right) d\theta$$

$$= \frac{1}{\pi} \int_0^{\pi/2} M_{\mu_{R_jD_k}} \left(-\frac{1}{\sin^2\theta} \right) M_{\mu_{S_iD_k}} \left(-\frac{1}{\sin^2\theta} \right) d\theta \quad (30)$$

where $M_\mu(\cdot)$ is the moment generating function (MGF) of μ, which is expressed as $M_\mu(s) = \mathbb{E}_\mu[e^{s\mu}]$. And the expressions of $M_{\mu_{R_jD_k}}(s)$ and $M_{\mu_{S_iD_k}}(s)$ are given in Eq. (31) and Eq. (32), respectively.

$$M_{\mu_{R_jD_k}} (s) = \int_0^\infty \exp \left(s\mu_{R_jD_k} \right) \frac{1}{\mu_{R_jD_k}\sqrt{8\pi\sigma_{R_jD_k}^2}} \exp \left\{ -\frac{\left[\ln\mu_{R_jD_k} - u_{R_jD_k} \right]^2}{8\sigma_{R_jD_k}^2} \right\} d\mu_{R_jD_k} \quad (31)$$

$$M_{\mu_{S_iD_k}} (s) = \int_0^\infty \exp \left(s\mu_{S_iD_k} \right) \frac{1}{\mu_{S_iD_k}\sqrt{8\pi\sigma_{S_iD_k}^2}} \exp \left\{ -\frac{\left[\ln\mu_{S_iD_k} - u_{S_iD_k} \right]^2}{8\sigma_{S_iD_k}^2} \right\} d\mu_{S_iD_k} \quad (32)$$

$u_{R_jD_k}$ and $u_{S_iD_k}$ are donated as $u_{R_jD_k} = \ln\bar{\mu} + 2\ln\overline{BSF_{R_jD_k}}(\delta, z_{rec}) - \sigma_{R_jD_k}^2$ and $u_{S_iD_k} = \ln\bar{\mu} + 2\ln\overline{BSF_{S_iD_k}}(\delta, z_{rec}) - \sigma_{S_iD_k}^2$, respectively. Furthermore, the Eq. (30) can be well approximated by employing the following relation [50, Eq. (10)]

$$P_{ABER}^{coop} \left(e | \mu_{S_iR_j} > SNR_{sr} \right) \approx \frac{1}{12} M_{\mu_{coop}} (-1) + \frac{1}{4} M_{\mu_{coop}} \left(-\frac{4}{3} \right). \quad (33)$$

With the help of the Gauss-Hermite quadrature formula in [48], the closed-form expression of the error probability in the cooperative case can be expressed as

$$P_{ABER}^{coop}\left(e|\,\mu_{S_iR_j} > SNR_{sr}\right) \approx \frac{1}{12}M_{\mu_{coop}}(-1) + \frac{1}{4}M_{\mu_{coop}}\left(-\frac{4}{3}\right)$$

$$= \frac{1}{12}\left\{\sum_{l_2=1}^{L_2}H_{l_2} \times \frac{1}{\sqrt{\pi}}\exp\left\{\exp\left(\sqrt{8\sigma_{S_iD_k}^2}a_{l_2} + u_{S_iD_k}\right) \times (-1)\right\}\right\}$$

$$\times \left\{\sum_{l_3=1}^{L_3}H_{l_3} \times \frac{1}{\sqrt{\pi}}\exp\left\{\exp\left(\sqrt{8\sigma_{R_jD_k}^2}a_{l_3} + u_{R_jD_k}\right) \times (-1)\right\}\right\}$$

$$+ \frac{1}{4}\left\{\sum_{l_2=1}^{L_2}H_{l_2} \times \frac{1}{\sqrt{\pi}}\exp\left\{\exp\left(\sqrt{8\sigma_{S_iD_k}^2}a_{l_2} + u_{S_iD_k}\right) \times \left(-\frac{4}{3}\right)\right\}\right\}$$

$$\times \left\{\sum_{l_3=1}^{L_3}H_{l_3} \times \frac{1}{\sqrt{\pi}}\exp\left\{\exp\left(\sqrt{8\sigma_{R_jD_k}^2}a_{l_3} + u_{R_jD_k}\right) \times \left(-\frac{4}{3}\right)\right\}\right\} \quad (34)$$

There still exists a decision error when the relay R_j transmits an incorrect signal to the destination D_k, even if the relay measures the quality of the received signal before forwarding it [46]. The conditional error propagation probability can be derived as

$$P_{ABER}^{prop}\left(e|\,\mu_{S_iR_j} > SNR_{sr}\right) = P_{ABER}^{prop}(e)$$

$$= \int_0^\infty \int_0^\infty \frac{1}{2}erfc\left(\frac{\mu_{S_iD_k} - \mu_{R_jD_k}}{\sqrt{\mu_{S_iD_k} + \mu_{R_jD_k}}}\right)f_{S_iD_k}\left(\mu_{S_iD_k}\right)f_{R_jD_k}\left(\mu_{R_jD_k}\right)d\mu_{S_iD_k}d\mu_{R_jD_k}$$

$$(35)$$

The proof of Eq. (35) is presented in Appendix A. With the help of Gauss-Hermite quadrature numerical method, the closed-form expression of $P_{ABER}^{prop}(e|\mu_{S_iR_j} > SNR_{sr})$ could be approximated as

$$P_{ABER}^{prop}\left(e|\,\mu_{S_iR_j} > SNR_{sr}\right) \approx \sum_{l_4=1}^{L_4}\sum_{l_5=1}^{L_5}\frac{1}{2\pi}H_{l_4}H_{l_5}$$

$$\times erfc\left(\frac{\exp\left(\sqrt{8\sigma_{S_iD_k}^2}a_{l_4} + u_{S_iD_k}\right) - \exp\left(\sqrt{8\sigma_{R_jD_k}^2}a_{l_5} + u_{R_jD_k}\right)}{\sqrt{\exp\left(\sqrt{8\sigma_{S_iD_k}^2}a_{l_4} + u_{S_iD_k}\right) + \exp\left(\sqrt{8\sigma_{R_jD_k}^2}a_{l_5} + u_{R_jD_k}\right)}}\right) \quad (36)$$

where a_{l_4} and a_{l_5} are the roots of Herimte quadrature, which is given in [48], H_{l_4} and H_{l_5} are the corresponding weighs, L_4 and L_5 are the number of points. Finally, submitting the Eq. (22), Eq. (23), Eq. (27), Eq. (34) and Eq. (36) into the Eq. (19), the accurately and effectively closed-form conditional ABER expressions of the cooperative optical IoUT system in DF mode could be achieved. When the instantaneous SNR of $S_i - R_j$ link is not more than SNR_{sr}, the cooperative optical IoUT system operates in AF mode. The equivalent end-to-end SNR of $S_i - R_j - D_k$ link can be expressed as

$$\mu_{eq} = \frac{\mu_{S_iR_j}\mu_{R_jD_k}}{\mu_{S_iR_j} + \mu_{R_jD_k} + 1} \approx \frac{\mu_{S_iR_j}\mu_{R_jD_k}}{\mu_{S_iR_j} + \mu_{R_jD_k}} \quad (37)$$

However, the above expression is not mathematically tractable. So the well-known inequality between geometric and harmonic means is adopted. For $x_1, x_2, \ldots, x_N$, $\mathcal{H}_N \leq \mathcal{G}_N$ holds on, where $\mathcal{H}_N \triangleq N(\sum_{i=1}^N x_i^{-1})^{-1}$ and $\mathcal{G}_N \triangleq \prod_{i=1}^N x_i^{1/N}$ are the harmonic and geometric means, respectively.

When $x_1 = x_2 = \ldots x_N$, the expression $\mathcal{H}_N = \mathcal{G}_N$ holds on. So an upper bound of μ_{eq} can be obtained

$$\mu_{eq} \approx \frac{1}{2}\left(\mu_{S_iR_j}\mu_{R_jD_k}\right)^{1/2} \tag{38}$$

Using the same method as Eq. (33), the ABER of the cooperative optical IoUT system in the case of AF strategy is given by

$$P_{ABER}^{AF}\left(e\mid \mu_{S_iR_j} \leq SNR_{sr}\right) \approx \frac{1}{12}M_{\mu_{AF}}(-1) + \frac{1}{4}M_{\mu_{AF}}\left(-\frac{4}{3}\right)$$

$$= \frac{1}{12}M_{\mu_{S_iD_k}}(-1)M_{\mu_{eq}}(-1) + \frac{1}{4}M_{\mu_{S_iD_k}}\left(-\frac{4}{3}\right)M_{\mu_{eq}}\left(-\frac{4}{3}\right) \tag{39}$$

$M_{\mu_{S_iD_k}}(s)$ is given in Eq. (32), and the expression of $M_{\mu_{eq}}(s)$ is given in Eq. (40). The detailed derivation process of $f_{\mu_{eq}}(z\mid \mu_{S_iR_j} \leq SNR_{sr})$ in Eq. (40) is shown in Appendix B.

$$M_{\mu_{eq}}(s) = \int_0^\infty \exp(sz) f_{\mu_{eq}}\left(z\mid \mu_{S_iR_j} \leq SNR_{sr}\right) dz$$

$$= \int_0^\infty \exp(sz) \frac{1}{P\left(\mu_{S_iR_j} \leq SNR_{sr}\right)} \frac{1}{\sqrt{2\pi\sigma_z^2}z} \exp\left(-\frac{1}{2}\frac{(\ln z + \ln 2 - u_z)^2}{\sigma_z^2}\right)$$

$$\times \left\{1 - \frac{1}{2}erfc\left(\left[\sqrt{\frac{\sigma_z^2}{\sigma_x^2\sigma_y^2}}\ln\sqrt{SNR_{sr}} - \frac{u_x\sigma_y^2 + \sigma_x^2(\ln z + \ln 2) - u_y\sigma_x^2}{\sqrt{\sigma_x^2\sigma_y^2\sigma_z^2}}\right]\Big/\sqrt{2}\right)\right\} dz \tag{40}$$

where $u_x = u_{S_iR_j}/2$, $u_y = u_{R_jD_k}/2$, $u_z = u_{S_iR_j}/2 + u_{R_jD_k}/2$, $\sigma_z^2 = \sigma_{R_jD_k}^2 + \sigma_{S_iR_j}^2$, $\sigma_x^2 = \sigma_{S_iR_j}^2$, $\sigma_y^2 = \sigma_{R_jD_k}^2$. Submitting Eq. (32) and Eq. (40) into Eq. (39), the closed-form expression of $P_{ABER}^{AF}(e\mid \mu_{S_iR_j} \leq SNR_{sr})$ can be obtained with the Gauss-Hermite quadrature numerical methods. It is as follows

$$P_{ABER}^{AF}\left(e\mid \mu_{S_iR_j} \leq SNR_{sr}\right) = \frac{1}{\frac{1}{2} + \frac{1}{2}erf\left\{\left[\ln(SNR_{sr}) - u_{S_iR_j}\right]\Big/\sqrt{8\sigma_{S_iR_j}^2}\right\}}$$

$$\times \left\{\begin{array}{l} \frac{1}{12} \times \sum_{l_6=1}^{L_6} H_{l_6} \times \frac{1}{\sqrt{\pi}}\exp\left[(-1) \times \exp\left(\sqrt{2\sigma_z^2}a_{l_6} + u_z - \ln 2\right)\right] \\ \times \left\{1 - \frac{1}{2}erfc\left(\left[\sqrt{\frac{\sigma_z^2}{\sigma_x^2\sigma_y^2}}\ln\sqrt{SNR_{sr}} - \frac{u_x\sigma_y^2 + \sigma_x^2\left(\sqrt{2\sigma_z^2}a_{l_6} + u_z\right) - u_y\sigma_x^2}{\sqrt{\sigma_x^2\sigma_y^2\sigma_z^2}}\right]\Big/\sqrt{2}\right)\right\} \\ \times \sum_{l_7=1}^{L_7} H_{l_7} \times \frac{1}{\sqrt{\pi}}\exp\left[(-1) \times \exp\left(\sqrt{8\sigma_z^2}a_{l_7} + u_{S_iD_k}\right)\right] \\ + \frac{1}{4} \times \sum_{l_6=1}^{L_6} H_{l_6} \times \frac{1}{\sqrt{\pi}}\exp\left[\left(-\frac{4}{3}\right) \times \exp\left(\sqrt{2\sigma_z^2}a_{l_6} + u_z - \ln 2\right)\right] \\ \times \left\{1 - \frac{1}{2}erfc\left(\left[\sqrt{\frac{\sigma_z^2}{\sigma_x^2\sigma_y^2}}\ln\sqrt{SNR_{sr}} - \frac{u_x\sigma_y^2 + \sigma_x^2\left(\sqrt{2\sigma_z^2}a_{l_6} + u_z\right) - u_y\sigma_x^2}{\sqrt{\sigma_x^2\sigma_y^2\sigma_z^2}}\right]\Big/\sqrt{2}\right)\right\} \\ \times \sum_{l_7=1}^{L_7} H_{l_7} \times \frac{1}{\sqrt{\pi}}\exp\left[\left(-\frac{4}{3}\right) \times \exp\left(\sqrt{8\sigma_z^2}a_{l_7} + u_{S_iD_k}\right)\right] \end{array}\right\} \tag{41}$$

3.2 Outage Probability

The outage probability is an important performance indicator to characterize the performance of cooperative relaying networks. It is defined as the probability that the instantaneous end-to-end SNR of the cooperative optical IoUT system falls below a predefined threshold μ_{th}. For the considered cooperative optical IoUT system with HDAF strategy, the outage probability can be

defined as

$$P_{OP}^{HDAF} = P\left(\mu_{S_iR_j} > SNR_{sr}\right) P_{DF}\,(outage) + P\left(\mu_{S_iR_j} \le SNR_{sr}\right) P_{AF}\,(outage), \tag{42}$$

where $P_{DF}(outage)$ is the probability that an outage event occurs after the destination combines the signals from the source and the relay, when the relay adopts DF strategy. While $P_{AF}(outage)$ denotes the probability of an outage event at destination when $\mu_{S_iR_j} \le SNR_{sr}$ holds on. In DF mode, the outage probability of the cooperative IoUT system can be calculated by

$$
\begin{aligned}
P_{OP}^{DF}\,(outage) &= P\left(\mu_{DF} < \mu_{th}\,|\,\mu_{S_iR_j} > SNR_{sr}\right) \\
&= P\left(\min\left\{\mu_{S_iR_j}, \mu_{R_jD_k} + \mu_{S_iD_k}\right\} < \mu_{th}\,\middle|\,\mu_{S_iR_j} > SNR_{sr}\right) \\
&= P\left(\mu_{R_jD_k} + \mu_{S_iD_k} < \mu_{th}\right) \\
&= \int_0^{\mu_{th}} f_{\mu_{R_jD_k}}(x) \int_0^{\mu_{th}-x} f_{\mu_{S_iD_k}}(y)\,dy\,dx \\
&= \int_0^{\mu_{th}} \frac{1}{x\sqrt{8\pi\sigma_{R_jD_k}^2}} \exp\left\{-\frac{[\ln x - u_{R_jD_k}]^2}{8\sigma_{R_jD_k}^2}\right\} \times \left\{\frac{1}{2} + \frac{1}{2}erf\left[\frac{\log(\mu_{th}-x) - u_{S_iD_k}}{\sqrt{8\sigma_{S_iD_k}^2}}\right]\right\} dx
\end{aligned}
\tag{43}
$$

In AF mode, the outage probability of the cooperative optical IoUT system can be expressed as

$$P_{OP}^{AF}\left(\mu_{AF} < \mu_{th}\,|\,\mu_{S_iR_j} \le SNR_{sr}\right)$$

$$
\begin{aligned}
&= P\left\{\mu_{S_iD_k} + \underbrace{\frac{1}{2}\left(\mu_{S_iR_j}\mu_{R_jD_k}\right)^{1/2}}_{\mu_{eq}} < \mu_{th}\,\middle|\,\mu_{S_iR_j} \le SNR_{sr}\right\} \\
&= \int_0^{\mu_{th}} f_{\mu_{eq}}\left(z\,|\,\mu_{S_iR_j} \le SNR_{sr}\right) \int_0^{\mu_{th}-z} f_{\mu_{S_iD_k}}(y)\,dy\,dz \\
&= \frac{1}{P\left(\mu_{S_iR_j} \le SNR_{sr}\right)} \int_0^{\mu_{th}} \left\{\frac{1}{2} + \frac{1}{2}erf\left[\frac{\log(\mu_{th}-z) - u_{S_iD_k}}{\sqrt{8\sigma_{S_iD_k}^2}}\right]\right\} \\
&\quad \times \frac{1}{\sqrt{2\pi\sigma_z^2}z}\exp\left[-\frac{1}{2}\frac{(\ln z + \ln 2 - u_z)^2}{\sigma_z^2}\right] \\
&\quad \times \left\{1 - \frac{1}{2}erfc\left(\left[\sqrt{\frac{\sigma_z^2}{\sigma_x^2\sigma_y^2}}\ln\sqrt{SNR_{sr}} - \frac{u_x\sigma_y^2 + \sigma_x^2(\ln z + \ln 2) - u_y\sigma_x^2}{\sqrt{\sigma_x^2\sigma_y^2\sigma_z^2}}\right]\middle/\sqrt{2}\right)\right\} dy
\end{aligned}
\tag{44}
$$

Then, the Eq. (43) and Eq. (44) can be solved with Gauss-Legendre quadrature rules. Finally, the outage probability expressions of the cooperative optical IoUT system in DF mode and AF mode are obtained as Eq. (45) and Eq. (46), respectively.

$$P_{OP}^{DF}\left(\mu_{end}^{DF} < \mu_{th}\,\middle|\,\mu_{S_iR_j} < SNR_{sr}\right)$$

$$= \frac{\mu_{th}}{2}\sum_{k_2=1}^{n_2} S_{k_2}\frac{1}{\omega_{k_2}\sqrt{8\pi\sigma_{R_jD_k}^2}}\exp\left\{-\frac{\left[\ln\left(\frac{\mu_{th}}{2} + \frac{\mu_{th}}{2}\times\omega_{k_2}\right) - u_{R_jD_k}\right]^2}{8\sigma_{R_jD_k}^2}\right\}$$

$$\times \left\{ \frac{1}{2} + \frac{1}{2} erf \left[\frac{\log\left(\frac{\mu_{th}}{2} - \frac{\mu_{th}}{2} \times \omega_{k_2}\right) - u_{S_i D_k}}{\sqrt{8\sigma_{S_i D_k}^2}} \right] \right\} \tag{45}$$

$$P_{OP}^{AF}\left(\mu_{end}^{AF} < \mu_{th} \middle| \mu_{S_i R_j} \leq SNR_{sr}\right)$$

$$= \frac{\mu_{th}}{2P\left(\mu_{S_i R_j} \leq SNR_{sr}\right)} \sum_{k_3=1}^{n_3} S_{k_3} \times \left\{ \frac{1}{2} + \frac{1}{2} erf \left[\frac{\log\left(\mu_{th}/2 - \mu_{th}/2 \times \omega_{k_3}\right) - u_{S_i D_k}}{\sqrt{8\sigma_{S_i D_k}^2}} \right] \right\}$$

$$\times \frac{1}{\sqrt{2\pi\sigma_z^2}\left(\mu_{th}/2 + \mu_{th}/2 \times \omega_{k_3}\right)} \exp\left\{ -\frac{\left[\ln\left(\mu_{th}/2 + \mu_{th}/2 \times \omega_{k_3}\right) + \ln 2 - u_z\right]^2}{2\sigma_z^2} \right\}$$

$$\times \left\{ 1 - \frac{1}{2} erfc \left(\left[\sqrt{\frac{\sigma_z^2}{\sigma_x^2 \sigma_y^2}} \ln\sqrt{SNR_{sr}} - \frac{u_x \sigma_y^2 + \sigma_x^2\left[\ln\left(\frac{\mu_{th}}{2} + \frac{\mu_{th}}{2}\omega_{k_3}\right) + \ln 2\right] - u_y \sigma_x^2}{\sqrt{\sigma_x^2 \sigma_y^2 \sigma_z^2}} \right] \middle/ \sqrt{2} \right) \right\} \tag{46}$$

where ω_{k_2}, ω_{k_3} are the roots of Legendre quadrature. S_{k_2} and S_{k_3} are the corresponding weight coefficients, which can be calculated by the Eq. (25). n_2 and n_3 are the numbers of points (expressions). Submitting Eq. (17), Eq. (18), Eq. (45) and Eq. (46) into Eq. (42), the closed-form expression of the outage probability for the cooperative optical HDAF-IoUT system over the aggregated UWOC channel is got.

4. Numerical Results and Discussions

In this section, the analytical and numerical simulation results are given to investigate the performance of the three-node half-duplex cooperative optical IoUT system with HDAF strategy over the UWOC fading channel, which fully considers the impact of absorption, scattering, link misalignment and oceanic turbulence. The analytical expressions of ABER and outage probability for the optical HDAF-IoUT system are obtained from Eq. (16) and Eq. (42). With the help of Gauss-Hermite and Gauss-Legendre quadrature rules, the accurately and effectively closed-form expressions of ABER and outage probability are obtained. n_1, n_2, n_3 and L_J, $J = 1, 2, \ldots, 7$, are chosen to be 30 in computing the Gauss-Legendre and Gauss-Hermite approximations, which are sufficient for the series to converge. The distance of the $S_i - R_j - D_k$ and $S_i - D_k$ links are assumed to be 10 m and 9 m, respectively. The distance between the source and relay is denoted by $d_{S_i R_j}$. We also assume that $P_S = \vartheta P'$, $P_R = (1 - \vartheta)P'$, where ϑ is the power allocation factor. Without loss of generality, each hop link is considered to be independent and identically distributed.

Fig. 3 shows the ABER curves of the cooperative optical IoUT system with HDAF strategy against the average SNR over the composite UWOC fading channels in different waters. We also provide the ABER performance of the cooperative optical IoUT systems based on FAF strategy, FDF strategy and point-to-point IoUT system for comparison. The point-to-point IoUT system adopts direct transmission (DT) scheme. The absorption and scattering coefficients for different waters are given in Table 1. As can be seen, the analytical results have excellent agreements with MC simulations with the increase of average SNR, which confirms the correctness of our theoretical ABER models. However, for the low SNR, the simulation and theoretical results are not matching very well. This phenomenon happens due to the approximate calculation of the integral of the MGF in Eq. (33) and Eq. (39). In weak oceanic turbulence, to achieve an ABER value of 10^{-6}, the cooperative optical HDAF-IoUT system requires 17 dB in pure water, 22 dB in clear water, and 34.2 dB in costal water. This is obvious, the fading effects caused by the absorption, scattering and link misalignment increase with the increase of the seawater turbidity, which immensely degrade the system performance. Furthermore, the cooperative optical HDAF-IoUT system is superior to the FAF-IoUT and the point-to-point IoUT systems in these three waters. For example, to achieve
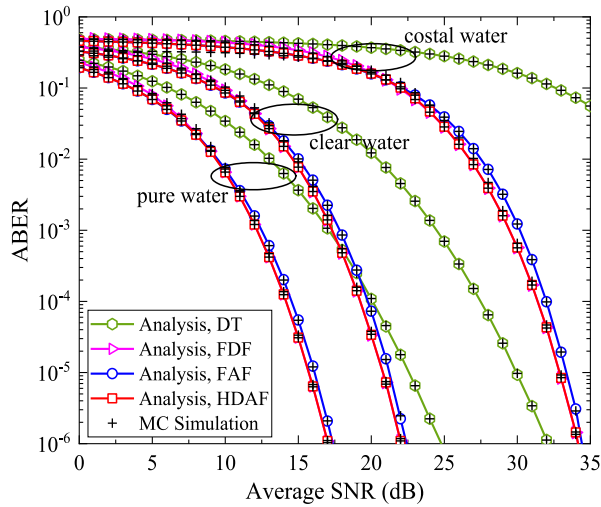
Fig. 3. ABER against the average SNR for the cooperative optical IoUT systems with HDAF, FDF, FAF strategies and point-to-point IoUT system in different waters.
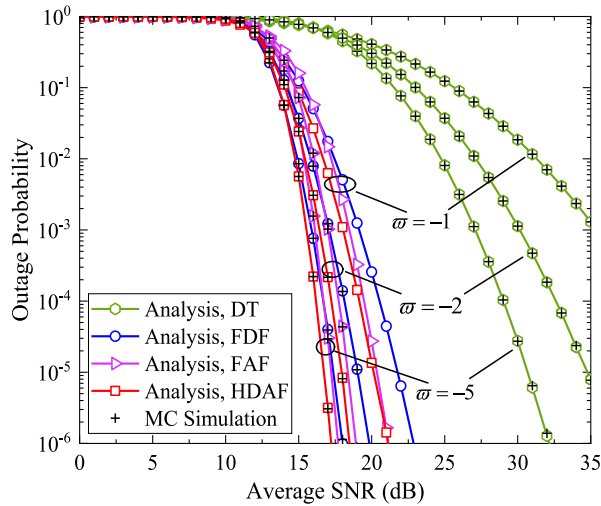

Fig. 4. Outage probability along with ϖ for the cooperative optical IoUT systems employing HDAF, FDF, FAF strategies and point-to-point IoUT system.

an ABER value of 10^{-5} in clear water, the HDAF-IoUT system requires 20.8 dB of SNR, the FAF-IoUT system and point-to-point IoUT system require 21.3 dB and 30 dB, respectively. And in high SNR region, the cooperative optical IoUT system with HDAF strategy almost has the same ABER performance with the FDF-IoUT system. This is because that the relay in HDAF strategy mainly employs the DF strategy to transmit the message when the instantaneous SNR of the $S_i - R_j$ link is large. In this case, it is almost consistent with the optical IoUT system with FDF strategy.

Fig. 4 demonstrates the outage probability as a function of the average SNR for the cooperative optical HDAF-IoUT, FDF-IoUT, FAF-IoUT systems and point-to-piont IoUT systems over the aggregated UWOC fading channels. As can be seen, the excellent match between the analytical and simulation results corroborates the accuracy of our derived analytical expressions of the outage probability for the cooperative optical HDAF-IoUT system. For different values of the relative
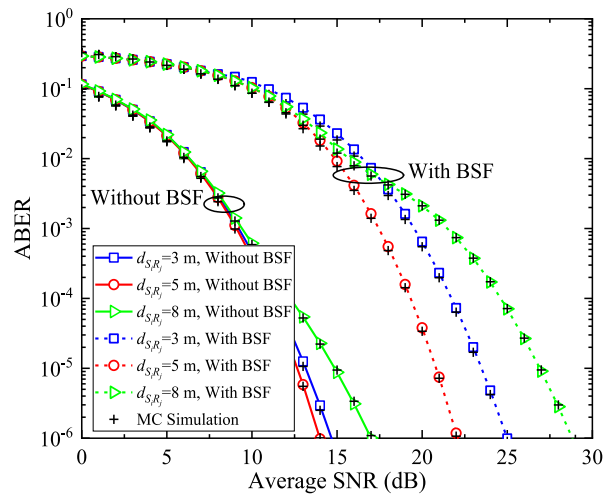
Fig. 5. ABER versus the average SNR for the HDAF-IoUT system with and without BSF.

strength of temperature and salinity fluctuations $\varpi = -1$, -3 and -5, the corresponding scintillation indexes of $S_i - R_j$ link are $\sigma_I^2(D)$ =0.3858, 0.2058, 0.1248, respectively. It can be found that the outage probability values of these four systems would shift to lower values with the decrease of the ϖ. This is a consequence of the scintillation index varying with the relative strength of temperature and salinity fluctuations. It indicates that the outage probability performance of these systems is enhanced with the decrease of the turbulence strengths. In addition, the cooperative optical HDAF-IoUT system has the lowest outage probability value for a fixed SNR gain comparing with those systems based on FDF and FAF strategies. Numerical speaking, for $\varpi = -2$, the HDAF-IoUT, FDF-IoUT and FAF-IoUT systems require 18.5 dB, 20.0 dB and 19.0 dB of SNR, respectively, to achieve an outage probability value of 10^{-6}. And the point-to-point IoUT system requires more than 35 dB SNR gain. This is reasonable, the cooperative optical IoUT system exploits the diversity provided in relay-assisted system, i.e., if the direct link transmission to the destination is failed, the signal could still be received at the destination through the relay-assisted link. What's more, the relay-assisted link divides the long transmitting distance into two shorter hops, the effects of absorption, scattering, link misalignment and oceanic turbulence of each hop would reduce greatly. And hence the cooperative optical IoUT system gets a much better performance.

Fig. 5 depicts the ABER performance of the cooperative optical HDAF-IoUT system with and without the consideration of BSF model when the relay locates in different positions with $d_{S_iR_j} =$ 3 m, $d_{S_iR_j} = 5$ m and $d_{S_iR_j} = 8$ m. The distance between the source node and the destination node is 9 m. The distance between the relay node and the destination node is 7 m, 5 m and 8 m, respectively. The BSF characterizes the effects of the absorption, scattering and link misalignment on the UWOC link. The power allocation factor is set to be 0.7. Expectedly, it can be observed that the ABER performance of the cooperative optical HDAF-IoUT systems with BSF are worse than those systems in the absence of BSF. When the distance between the source node and the relay node is 3 m, to achieve an ABER value of 10^{-6}, the cooperative optical HDAF-IoUT system without BSF requires 14.0 dB of SNR, while the system with the consideration of BSF requires 22.2 dB of SNR. It indicates that the absorption, scattering and link misalignment would have a substantial impact on the UWOC systems, which are extremely important factors while modeling and simulating the underwater communication channel. In addition, whether the BSF is considered, the cooperative optical HDAF-IoUT system has a better ABER performance when the relay is close to the middle position between the S_i and R_j. For instance, at an average SNR $\bar{\mu} = 22$dB, the ABER value of the optical HDAF-IoUT system with $d_{S_iR_j} = 5$ m equals 1.07×10^{-6} and the values
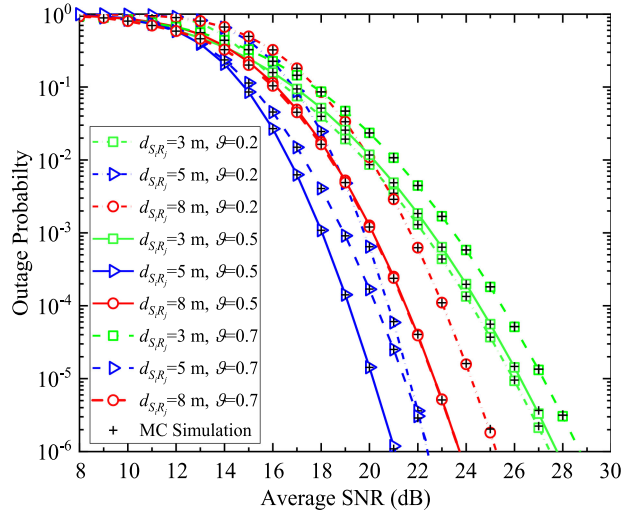
Fig. 6. Outage probability of the cooperative optical HDAF-IoUT system with respect to average SNR for different power allocation factor ϑ and $d_{S_i R_j}$.

of those systems with $d_{S_i R_j} = 3$m and $d_{S_i R_j} = 8$m are 1.97×10^{-4} and 0.0013, respectively. This can be explained by the fact that as the relay R_j is close to S_i, the probability of the relay operating in DF mode increases. However, the channel condition of the relay to the destination is poor, which would result that the error probability from the relay to the destination increases. As R_j is close to D_k, the channel condition of the source to the relay is poor, the probability of error propagation event would increase.

In Fig. 6, the outage probability of the cooperative optical HDAF-IoUT system with BSF versus the average SNR is presented in clear water with different power allocation factors ($\vartheta = 0.2$, $\vartheta = 0.5$ and $\vartheta = 0.7$), when the relay R_j is located in different positions $d_{S_i R_j} = 3$ m, $d_{S_i R_j} = 5$ m and $d_{S_i R_j} = 8$ m. For the sake of clarity, only the region of average SNR greater than or equal to 8 dB is plotted. As is seen from this figure, the power allocation scheme has less impact on the performance of the cooperative optical HDAF-IoUT system than the relay location. When the relay is close to the source, the cooperative optical HDAF-IoUT system has a better outage performance with the low power allocation scheme, e.g., $\vartheta = 0.2$. When the relay is close to the destination, the cooperative optical HDAF-IoUT system would outperform with the high power allocation strategy, e.g., $\vartheta = 0.7$. This phenomenon can be explained as follows. The absorption, scattering, link misalignment and oceanic turbulence *et al.* impairing effects would be more serious with the increase of link distance [51]. And the system requires to allocate more power for the node, which is equipped with longer transmitting distance, to resist the performance degradation caused by those impairing effects. Additionally, the cooperative optical HDAF-IoUT system earns better outage performance when the relay is close to the middle location for these three power allocation schemes.

Fig. 7 displays the variation curves of the ABER and outage probability of the cooperative optical HDAF-IoUT system with the average SNR over the aggregated lognormal and EGG fading channels. The absorption, scattering and link misalignment are described by BSF. The distances of $S_i - R_j$, $R_j - D_k$, $S_i - D_k$ links are assumed to be 1 m [23]. For a fair comparison, the turbulence parameters for both distributions are set to be the same values, i.e., $\sigma_I^2(D) = 3.6044 \times 10^{-4}$, and the level of air bubbles BL $= 0$L/min. Numerical results show that whether the BSF is considered, the cooperative optical HDAF-IoUT system over the aggregated EGG fading channel almost has the same ABER and outage probability values as that of the system over the aggregated lognormal fading channel, respectively, when the scintillation index is 3.6044×10^{-4}. Furthermore, one can note that for the case of $\sigma_I^2(D) = 0.1088$ and BL $= 2.4$L/min, the ABER performance and outage performance under the aggregated lognormal fading channel will outperform their EGG
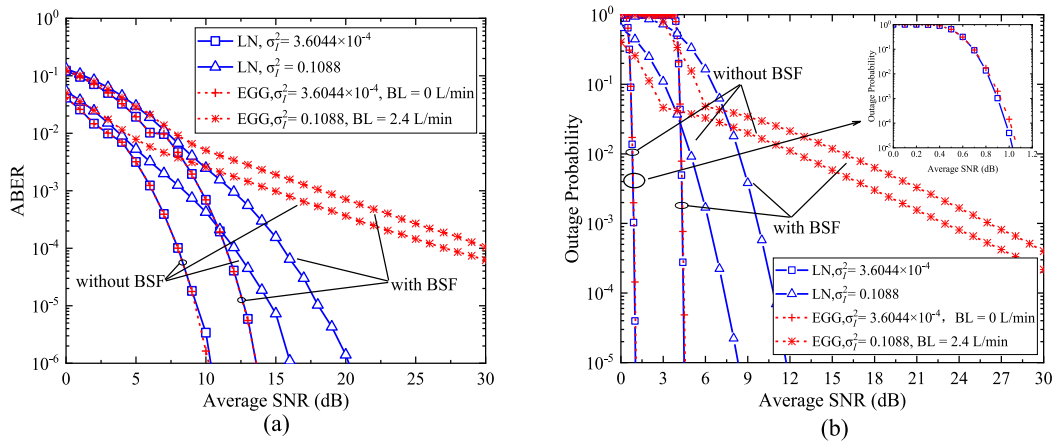
Fig. 7. Contrast between the aggregated EGG and lognormal channels (a) ABER (b) Outage probability.

counterpart, respectively. This is because the mixed EGG distribution is a comprehensive channel model, in which the effects of air bubbles and temperature gradient are comprehensively included [52]. While because the mixed EGG distribution has been developed in a 1m × 0.6m × 0.6m water tank, the parameters available from the experiments are quite limited [23]. Thus, the lognormal fading channel model is often adopted to investigate the wireless optical communication systems in underwater environment over a relatively long transmitting distance [18], [19], [22].

5. Conclusion

In this work, a cooperative optical IoUT system with HDAF strategy was presented and investigated over the aggregated lognormal fading channel. Specially, the BSF model was adopted to character-ize the fading effects including the absorption, scattering and link misalignment caused by spatial spreading in the seawater. On the basis of Gauss-Hermite quadrature criterion, Gauss-Legendre quadrature criterion and the properties of lognormal random variables, the closed-form ABER and outage probability expressions of the cooperative optical HDAF-IoUT system were derived math-ematically and confirmed by MC simulations. Moreover, an in-depth study of the effects of power allocation schemes and relay locations on the ABER and outage probability performance of the HDAF-IoUT system were also given. The analysis and simulation results show that the cooperative optical HDAF-IoUT system outperforms the FAF-IoUT and point-to-point IoUT systems over the aggregated lognormal fading channel. In the high SNR region, it almost has the same ABER performance with the cooperative optical FDF-IoUT system. While for a fixed power allocation scheme, the cooperative optical HDAF-IoUT system earns a better performance when the relay is close to the middle location of the relay-assisted link. This work will be of great help for the system design of cooperative optical IoUT networks over the UWOC fading channel.

Appendix A

The received signals at the destination when the relay adopts DF strategy can be expressed as

$$
\begin{aligned}
y_{D_k} &= w_{R_j D_k} y_{R_j D_k} + w_{S_i D_k} y_{S_i D_k} \\
&= w_{R_j D_k} \left(h_{R_j D_k} \hat{x} + n_{R_j D_k} \right) + w_{S_i D_k} \left(h_{S_i D_k} x + n_{S_i R_j} \right).
\end{aligned}
\tag{47}
$$

For BPSK, $\hat{x}$ at the relay can only take one of two values, $\hat{x} = x$ or $\hat{x} = -x$. For each value, the MRC output at the destination is

$$
y_{D_k} = \begin{cases} \left(w_{R_j D_k} h_{R_j D_k} + w_{S_i D_k} h_{S_i D_k} \right) x + \underbrace{w_{R_j D_k} n_{R_j D_k} + w_{S_i D_k} n_{S_i R_j}}_{n_{12}}, & \text{if } \hat{x} = x \\[4mm] \left(-w_{R_j D_k} h_{R_j D_k} + w_{S_i D_k} h_{S_i D_k} \right) x + \underbrace{w_{R_j D_k} n_{R_j D_k} + w_{S_i D_k} n_{S_i R_j}}_{n_{12}}, & \text{if } \hat{x} = -x \end{cases}, \tag{48}
$$

where n_{12} is a complex Gaussian random variable with zero mean and variance $\sigma_{12}^2 = (|w_{R_j D_k}|^2 + |w_{S_i D_k}|^2) N_0/2$. Since BPSK is real-valued, it suffices to consider only the real part $y = \text{Re}(y_{D_k})$ [53], which is a real Gaussian random variable with zero mean and variance $(|w_{R_j D_k}|^2 + |w_{S_i D_k}|^2) N_0/2$. When the relay decodes the received signals incorrectly, the PDF of y is given as

$$
f_y(y) = \begin{cases} \dfrac{1}{\sqrt{2\pi\sigma_{12}^2}} \exp\left\{ -\dfrac{\left(y - \left(-w_{R_j D_k} h_{R_j D_k} + w_{S_i D_k} h_{S_i D_k} \right) \right)^2}{2\sigma_{12}^2} \right\}, & \text{if } x = 1 \\[5mm] \dfrac{1}{\sqrt{2\pi\sigma_{12}^2}} \exp\left\{ -\dfrac{\left(y + \left(-w_{R_j D_k} h_{R_j D_k} + w_{S_i D_k} h_{S_i D_k} \right) \right)^2}{2\sigma_{12}^2} \right\}, & \text{if } x = 0 \end{cases}. \tag{49}
$$

Therefore, the error propagation probability in DF scheme can be calculated by

$$
p(e) = P(0) P(1|0) + P(1) P(0|1)
$$

$$
= \frac{1}{2} \times \int_0^{+\infty} f_y(y|x = 0) dy + \frac{1}{2} \times \int_{-\infty}^0 f_y(y|x = 1) dy. \tag{50}
$$

Submitting Eq. (49) into Eq. (50), the error propagation probability in terms of $\mu_{S_i D_k}$ and $\mu_{R_j D_k}$ can be obtained as

$$
p_{BER}^{prop}(e) = \frac{1}{2} Q\left(\frac{\left(|h_{S_i D_k}|^2 - |h_{R_j D_k}|^2 \right)}{\sqrt{\left(|h_{S_i D_k}|^2 + |h_{R_j D_k}|^2 \right) N_0/2}} \right) + \frac{1}{2}\left\{ 1 - Q\left(\frac{\left(|h_{R_j D_k}|^2 - |h_{S_i D_k}|^2 \right)}{\sqrt{\left(|h_{S_i D_k}|^2 + |h_{R_j D_k}|^2 \right) N_0/2}} \right) \right\}
$$

$$
= \frac{1}{2} \times \frac{1}{2} erfc\left(\frac{\mu_{S_i D_k} - \mu_{R_j D_k}}{\sqrt{\mu_{S_i D_k} + \mu_{R_j D_k}}} \right) + \frac{1}{2} \times \left\{ 1 - \frac{1}{2} erfc\left(\frac{\mu_{R_j D_k} - \mu_{S_i D_k}}{\sqrt{\mu_{S_i D_k} + \mu_{R_j D_k}}} \right) \right\}
$$

$$
= \frac{1}{2} erfc\left(\frac{\mu_{S_i D_k} - \mu_{R_j D_k}}{\sqrt{\mu_{S_i D_k} + \mu_{R_j D_k}}} \right). \tag{51}
$$

Taking expectation over $\mu_{S_i D_k}$ and $\mu_{R_j D_k}$ on both sides of Eq. (51), the average error propagation probability in DF scheme can be calculated by

$$
P_{ABER}^{prop}(e) = \int_0^\infty \int_0^\infty \frac{1}{2} erfc\left(\frac{\mu_{S_i D_k} - \mu_{R_j D_k}}{\sqrt{\mu_{S_i D_k} + \mu_{R_j D_k}}} \right) f_{S_i D_k}\left(\mu_{S_i D_k} \right) f_{R_j D_k}\left(\mu_{R_j D_k} \right) d\mu_{S_i D_k} d\mu_{R_j D_k}. \tag{52}
$$

Appendix B

According to the properties of lognormal random variables in [54], $x = \mu_{S_i R_j}^{1/2}$ is also a lognormal random variable with mean $u_x = u_{S_i R_j}/2$ and variance $\sigma_x^2 = \sigma_{S_i R_j}^2$. $y = \mu_{R_j D_k}^{1/2}$ is also a lognormal random variable with mean $y = \mu_{R_j D_k}^{1/2}$ and variance $\sigma_x^2 = \sigma_{R_j D_k}^2$. The PDFs of x and y can be expressed as

$$
f(x) = \frac{1}{\sqrt{2\pi\sigma_x^2} x} \exp\left(-\frac{(\ln x - u_x)^2}{2\sigma_x^2} \right), \tag{53}
$$

$$f(y) = \frac{1}{\sqrt{2\pi\sigma_y^2}y}\exp\left(-\frac{(\ln y - u_y)^2}{2\sigma_y^2}\right). \tag{54}$$

Considering $\mu_{S_iR_j} \leq SNR_{sr}$, it can infer that $x \leq a$, where $a = \sqrt{SNR_{sr}}$. The PDF of $z' = xy$ in AF strategy is given as Eq. (55), where $P(x \leq a) = P(\mu_{S_iR_j} \leq SNR_{sr})$. Since $\mu_{eq} = (\mu_{S_iR_j}\mu_{R_jD_k})^{1/2}/2 = xy/2$, the PDF of μ_{eq} can be obtained as Eq. (56).

$$\begin{aligned}
f_{XY}(z'|x \leq a) &= \frac{\partial}{\partial z}\left[\frac{P_{XY}(xy < z', x \leq a)}{P(x \leq a)}\right] \\
&= \frac{1}{P(x \leq a)}\int_0^a \frac{1}{x}f\left(x, \frac{z'}{x}\right)dx \\
&= \frac{1}{P(x \leq a)}\int_0^a \frac{1}{x}\frac{1}{\sqrt{2\pi\sigma_x^2}x}\exp\left(-\frac{(\ln x - u_x)^2}{2\sigma_x^2}\right) \\
&\quad \times \frac{1}{\sqrt{2\pi\sigma_y^2\frac{z'}{x}}}\exp\left(-\frac{(\ln z' - \ln x - u_y)^2}{2\sigma_y^2}\right)dx \\
&= \frac{1}{P(x \leq a)}\frac{1}{\sqrt{2\pi\left(\sigma_x^2 + \sigma_y^2\right)}z'}\exp\left(-\frac{1}{2}\frac{(\ln z' - (u_x + u_y))^2}{\left(\sigma_y^2 + \sigma_x^2\right)}\right) \\
&\quad \times \Phi\left(\sqrt{\frac{\sigma_y^2 + \sigma_x^2}{\sigma_x^2\sigma_y^2}}\ln a - \frac{u_x\sigma_y^2 + \sigma_x^2\ln z' - u_y\sigma_x^2}{\sqrt{\sigma_x^2\sigma_y^2\left(\sigma_y^2 + \sigma_x^2\right)}}\right).
\end{aligned} \tag{55}$$

$$\begin{aligned}
f_{\mu_{eq}}(z|\mu_{S_iR_j} \leq SNR_{sr}) &= \frac{1}{P\left(\mu_{S_iR_j} \leq SNR_{sr}\right)}\frac{1}{\sqrt{2\pi\sigma_z^2}z}\exp\left(-\frac{1}{2}\frac{(\ln z + \ln 2 - u_z)^2}{\sigma_z^2}\right) \\
&\quad \times \left\{1 - \frac{1}{2}erfc\left(\left[\sqrt{\frac{\sigma_z^2}{\sigma_x^2\sigma_y^2}}\ln\sqrt{SNR_{sr}} - \frac{u_x\sigma_y^2 + \sigma_x^2(\ln z + \ln 2) - u_y\sigma_x^2}{\sqrt{\sigma_x^2\sigma_y^2\sigma_z^2}}\right]\bigg/\sqrt{2}\right)\right\}.
\end{aligned} \tag{56}$$

References

[1] C. B. I. Trichili, B. S. Ooi, and M.-S. Alouini, "A CNN-based structured light communication scheme for internet of underwater things applications," *IEEE Internet Things J.,* vol. 7, no. 10, pp. 10038–10047, Oct. 2020.

[2] C. Zou, and F. Yang, "Autoencoder based underwater wireless optical communication with high data rate," *Opt. Lett.,* vol. 46, no. 6, pp. 1446–1449, 2021.

[3] R. P. N. Uppalapati, and P. Krishnan, "Analysis of M-QAM modulated underwater wireless optical communication system for reconfigurable UOWSNs employed in river meets ocean scenario," *IEEE Trans. Veh. Technol.,* vol. 69, no. 12, pp. 15244–15252, Dec. 2020.

[4] N. S. Celik, B. Shihada, T. Y. Al-Naffouri, and M.-S. Alouini, "A software-defined opto-acoustic network architecture for internet of underwater things," *IEEE Commun. Mag.,* vol. 58, no. 4, pp. 88–94, Apr. 2020.

[5] T. Nguyen, M. T. Nguyen, and V. V. Mai, "Underwater optical wireless communication-based IoUT networks: MAC performance analysis and improvement," *Opt. Switch. Netw.,* vol. 37, 2020, Art. no. 100570.

[6] N. Saeed, M. S. Alouini, and T. Y. Al-Naffouri, "Accurate 3D localization of selected smart objects in optical internet of underwater things," *IEEE Internet Things J.,* vol. 7, no. 2, pp. 937–947, Feb. 2020.

[7] Y. Zhou, and R. Diamant, "A parallel decoding approach for mitigating near-far interference in internet of underwater things," *IEEE Internet Things J.,* vol. 7, no. 10, pp. 9747–9759, Oct. 2020.

[8] Y. Song, "Underwater acoustic sensor networks with cost efficiency for internet of underwater things," *IEEE Trans. Ind. Electron.,* vol. 68, no. 2, pp. 1707–1716, Feb. 2021.

[9] X. Sun *et al.*, "A review on practical considerations and solutions in underwater wireless optical communication," *J. Lightw. Technol.*, vol. 38, no. 2, pp. 421–431, Jan. 2020.

[10] A. Uppalapati, R. P. Naik, and P. Krishnan, "Analysis of M-QAM modulated underwater wireless optical communication system for reconfigurable UOWSNs employed in river meets ocean scenario," *IEEE Trans. Veh. Technol.*, vol. 69, no. 12, pp. 15244–15252, Dec. 2020.

[11] S. A. Nezamalhosseini, and L. R. Chen, "Optimal power allocation for MIMO underwater wireless optical communication systems using channel state information at the transmitter," *IEEE J. Ocean. Eng.*, vol. 46, no. 3, pp. 319–325, Jan. 2021.

[12] S. K. Sahu, and P. Shanmugam, "A theoretical study on the impact of particle scattering on the channel characteristics of underwater optical communication system, optical communication," *Opt. Commun.*, vol. 408, pp. 3–14, 2017.

[13] S. Tang, Y. Dong, and X. Zhang, "Impulse response modeling for underwater wireless optical communication links," *IEEE Trans. Commun.*, vol. 62, no. 1, pp. 226–234, Jan. 2014.

[14] M. Elamassie, F. Miramirkhani, and M. Uysal, "Performance characterization of underwater visible light communication," *IEEE Trans. Commun.*, vol. 67, no. 1, pp. 543–552, Jan. 2019.

[15] M. Cochenour, L. J. Mullen, and A. E. Laux, "Characterization of the beam-spread function for underwater wireless optical communications links," *IEEE J. Ocean. Eng.*, vol. 33, no. 4, pp. 513–521, 2009.

[16] S. Tang, Y. Dong, and X. Zhang, "On link misalignment for underwater wireless optical communications," *IEEE Commun. Lett.*, vol. 16, no. 10, pp. 1688–1690, Oct. 2012.

[17] Y. Ata, and Y. Baykal, "Scintillations of optical plane and spherical waves in underwater turbulence," *J. Opt. Soc. Amer. A*, vol. 31, no. 7, pp. 1552–1556, 2014.

[18] X. Yi, Z. Li, and Z. Liu, "Underwater optical communication performance for laser beam propagation through weak oceanic turbulence," *Appl. Opt.*, vol. 54, no. 6, pp. 1273–1278, 2015.

[19] M. C. Gökçe, and Y. Baykal, "Aperture averaging and BER for Gaussian beam in underwater oceanic turbulence," *Opt. Commun.*, vol. 410, pp. 830–835, 2018.

[20] X. Luan, P. Yue, and X. Yi, "Scintillation index of an optical wave propagating through moderate-to-strong oceanic turbulence," *J. Opt. Soc. Amer. A*, vol. 36, no. 12, pp. 2048–2059, 2019.

[21] M. V. Jamali *et al.*, "Statistical studies of fading in underwater wireless optical channels in the presence of air bubble, temperature, and salinity random variations," *IEEE Trans. Commun.*, vol. 66, no. 10, pp. 4706–4723, Oct. 2018.

[22] M. V. Jamali, J. A. Salehi, and F. Akhoundi, "Performance studies of underwater wireless optical communication systems with spatial diversity: MIMO scheme," *IEEE Trans. Commun.*, vol. 65, no. 3, pp. 1176–1192, Mar. 2017.

[23] H. M. O. Zedini, A. Kammoun, M. Hamdi, B. S. Ooi, and M. Alouini, "Unified statistical channel model for turbulence-induced fading in underwater wireless optical communication systems," *IEEE Trans. Commun.*, vol. 67, no. 4, pp. 2893–2907, Apr. 2019.

[24] P. N. Ramavath, S. A. Udupi, and P. Krishnan, "High-speed and reliable underwater wireless optical communication system using multiple-input multiple-output and channel coding techniques for IoUT applications," *Opt. Commun.*, vol. 461, 2020, Art. no. 125229.

[25] M. Ferdaouss M, K. M. Ali, and B. Salah, "Improving the performance of underwater wireless optical communication links by channel coding," *Appl. Opt.*, vol. 57, no. 9, pp. 2115–2120, 2018.

[26] R. Li, J. Zhang, and A. Dang, "Cooperative system in free-space optical communications for simultaneous multiuser transmission," *IEEE Commun. Lett.*, vol, vol. 22, no. 10, pp. 2036–2039, Oct. 2018.

[27] J. N. Laneman, D. N. C. Tse, and G. W. Wornell, "Cooperative diversity in wireless networks: Efficient protocols and outage behavior," *IEEE Trans. Inf. Theory*, vol. 50, no. 12, pp. 3062–3080, Dec. 2004.

[28] H. Xiao, and S. Ouyang, "Power allocation for a hybrid decode-amplify-forward cooperative communication system with two source-destination pairs under outage probability constraint," *IEEE Syst. J.*, vol. 9, no. 3, pp. 797–804, Sep. 2015.

[29] P. A. Anghel, and M. Kaveh, "Exact symbol error probability of a cooperative network in a rayleigh-fading environment," *IEEE Trans. Wireless Commun.*, vol. 3, no. 5, pp. 1416–1421, Sep. 2004.

[30] G. Farhadi, and N. Beaulieu, "On the ergodic capacity of wireless relaying systems over rayleigh fading channels," *IEEE Trans. Wireless Commun.*, vol. 7, no. 11, pp. 4462–4467, Nov. 2008.

[31] S. S. Ikki, P. Ubaidulla, and S. Aissa, "Performance study and optimization of cooperative diversity networks with co-channel interference," *IEEE Trans. Wireless Commun.*, vol. 13, no. 1, pp. 14–23, Jan. 2014.

[32] A. Nasri, R. Schober, and I. F. Blake, "Performance and optimization of amplify-and-forward cooperative diversity systems in generic noise and interference," *IEEE Trans. Wireless Commun.*, vol. 10, no. 4, pp. 1132–1143, Apr. 2011.

[33] S. R, M. D. Selvaraj, and R. Roy, "Exact error analysis of MPAM signaling for a cooperative diversity system with correlated links using paired error approach," *IEEE Commun. Lett.*, vol. 18, no. 2, pp. 273–276, Feb. 2014.

[34] S. R, M. D. Selvaraj, and R. Roy, "On the error and outage performance of Decode-and-Forward cooperative selection diversity system with correlated links," *IEEE Trans. Veh. Technol.*, vol. 64, no. 8, pp. 3578–3593, Aug. 2015.

[35] M. Yu, and J. Li, "Is amplify-and-forward practically better than decode-and-forward or vice versa?," in *Proc. IEEE Int. Conf. Acoust., Speech, Signal Process.*, Philadelphia, PA, USA, Mar. 2005, pp. 365–368.

[36] F. A. Onat, A. Adinoyi, Y. Fan, H. Yanikomeroglu, J. S. Thompson, and I. D. Marsland, "Threshold selection for SNR-based selective digital relaying in cooperative wireless networks," *IEEE Trans. Wireless Commun.*, vol. 7, no. 11, pp. 4226–4237, Nov. 2008.

[37] R. Boluda-Ruiz, A. García-Zambrana, B. Castillo-Vázquez, and C. Castillo-Vázquez, "Impact of relay placement on diversity order in adaptive selective DF relay-assisted FSO communications," *Opt. Exp.*, vol. 23, no. 3, pp. 2600–2617, 2015.

[38] N. Varshney, A. V. Krishna, and A. K. Jagannatham, "Selective DF protocol for MIMO STBC based single/multiple relay cooperative communication: End-to-end performance and optimal power allocation," *IEEE Trans. Commun.*, vol. 63, no. 7, pp. 2458–2474, Jul. 2015.

[39] T. Q. Duong, and H. J. Zepernick, "On the performance gain of hybrid decode-amplify-forward cooperative communications," *EURASIP J. Wireless Comm. Netw.*, pp. 1–10, 2009.

[40] T. Q. Duong, and H. Zepernick, "Hybrid decode-amplify-forward cooperative communications with multiple relays," in *Proc. IEEE Wireless Commun. Netw. Conf.*, 2009, pp. 1–6.

[41] H. Xiao, Z. Zhang, and A. T. Chronopoulos, "Performance analysis of multi-source multi-destination cooperative vehicular networks with the hybrid decode-amplify-forward cooperative relaying protocol," *IEEE Trans. Intell. Transp. Syst.*, vol. 19, no. 9, pp. 3081–3086, Sep. 2018.

[42] H. Khanna, M. Aggarwal, and S. Ahuja, "Further results on the performance improvement in mixed RF-FSO systems using hybrid DF/AF (HDAF) relaying," *Trans. Emerg. Tel. Tech.*, vol. 29, no. 6, 2018, pp. Paper e3284.

[43] L. Xu, H. Zhang, and T. A. Gulliver, "Performance analysis of SNR-based HDAF M2M cooperative networks," *J. Elect. Comput. E.*, vol. 2015, pp. 1–7, 2015. [Online] Available: http://dx.doi.org/10.1155/2015/841937

[44] A. Salem, and L. Musavian, "NOMA in cooperative communication systems with energy-harvesting nodes and wireless secure transmission," *IEEE Trans. Wireless Commun.*, vol. 20, no. 2, pp. 1023–1037, Feb. 2021.

[45] Z. Zhou, B. Yao, R. Xing, and S. Bu, "E-CARP: An energy efficient routing protocol for UWSNs in the internet of underwater things," *IEEE Sensors J.*, vol. 16, no. 11, pp. 4072–4082, Jun. 2016.

[46] Z. Bai, J. Jia, and C. X. Wang, "Performance analysis of SNR-based incremental hybrid decode-amplify-forward cooperative relaying protocol," *IEEE Trans. Commun.*, vol. 63. no. 3, pp. 2094–2106, Jun. 2015.

[47] Y. Feng, S. Yan, Z. Yang, N. Yang, and W. Zhu, "TAS-based incremental hybrid decode–amplify–forward relaying for physical layer security enhancement," *IEEE Trans. Commun.*, vol. 65, no. 9, pp. 3876–3891, Sep. 2017.

[48] M. Abramowitz, and I. A. Stegun, *Handbook of Mathematical Functions With Formulas, Graphs, and Mathematical Tables*. New York, NY, USA: Dover, 1972.

[49] H. Ghavami, and S. S. Moghaddam, "Outage probability of device to device communications underlaying cellular network in suzuki fading channel," *IEEE Commun. Lett.*, vol. 21, no. 5, pp. 1203–1206, May 2017.

[50] M. Mckay, A. Zanella, and I. Collings, "Error probability and SINR analysis of optimum combining in rician fading," *IEEE Trans. Commun.*, vol. 57, no. 3, pp. 676–687, Mar. 2009.

[51] M. V. Jamali, A. Chizari, and A. S. Jawad, "Performance analysis of multi-hop underwater wireless optical communication systems," *IEEE Photon. Technol. Lett.*, vol. 29, no. 5, pp. 462–465, Mar. 2017.

[52] Y. Lou, R. Sun, J. Cheng, D. Nie, and G. Qiao, "Secrecy outage analysis of two-hop decode-and-forward mixed RF/UWOC systems," *IEEE Commun. Lett.*, to be published, doi: 10.1109/LCOMM.2021.3058988.

[53] T. Wang, A. Cano, G. B. Giannakis, and J. N. Laneman, "High-performance cooperative demodulation with decode-and-forward relays," *IEEE Trans. Commun.*, vol. 55, no. 7, pp. 1427–1438, Jul. 2007.

[54] E. L. Crow, K. Shimizu, *Lognormal Distributions: Theory and Applications*. New York, NY, USA: Marcel Dekker, 1987.